Coherent Optical CDMA with low MAI

A. Brinton Cooper, *Life Senior Member, IEEE,* Jacob B. Khurgin, Shuangmei Xu, and Jin U. Kang

***Abstract*—A novel coherent optical code division multiple access (OCDMA) network based on phase and polarization diversity balanced reception of spectrally encoded optical pulses is proposed. Spectral efficiencies of 1 bps/Hz and beyond can be achieved by minimizing multiple access interference (MAI) and by cancelling beat noise. While the system achieves full capacity under bit synchronism, it also offers competitive performance at up to 25% of full capacity, even when completely asynchronous. Tree and ring network configurations can assure synchronization, making the proposed system robust in the presence of dispersion and phase noise.**

I. Introduction

THE explosion of wireless, mobile communications is due largely to the use of code division multiple access (CDMA) waveforms that provide excellent spectral efficiency, system capacity, and signal quality and a degree of communications security. For decades, attempts to bring the benefits of CDMA to the fiber optic domain met with but modest success. In principle, optical CDMA (OCDMA) can provide wireless-like attributes (*e.g.,* asynchronous transmission, communications security, soft capacity on demand, and scalability) but radio frequency (RF) CDMA can directly measure the phase and amplitude of the received carrier, whereas optical components generally permit the direct measurement of intensity only. Thus, RF CDMA receivers can coherently process received signals, thereby suppressing the MAI from other user signals to very low levels. Conversely, the lack of coherent optical reception has limited OCDMA to using unsigned or sparse sequences with poor multiple access properties. When a broadband optical source is used, the resulting large *speckle* or *beat noise* [1] limits the system to just a few users [2]–[4].

In the proposed scheme, the diversity combining receiver offers nearly perfect orthogonality and complete cancellation of MAI and speckle noise, all of which are unattainable by other methods. The sensitivity of the output bit error rate *(b.e.r.)* to the number of active users offers a "fail-soft" capability. The virtual elimination of MAI also affords good spectral efficiency, system capacity, and *b.e.r,* as well as the means to implement strong communications security. Physical component impairments and bit-asynchronous reception cause elevations in MAI that are successfully handled.

Section II describes the system architecture and the key features of phase diversity reception that eliminate the need for phase locking. Section III discusses MAI modeling in order to estimate the impact of bit asynchronous reception. Section IV investigates constraints imposed by dispersion, nonlinearity, and laser line width and Section V offers conclusions.

Authors are with the Department of Electrical & Computer Engineering, The Johns Hopkins University, Baltimore, MD 21218

II. Basic Architecture

In the proposed design, (Figs. 1, 2), a single, mode-locked laser provides a stable, optical pulse train that, with gain equalization [5], produces a flat, optical comb spectrum that is split into M user streams. In each stream, the comb is spectrally demultiplexed into two combs comprising "odd" and "even" numbered lines, respectively[1]. Spectral phase coding (SPC)[2] of the demultiplexed spectrum by symbols from a Hadamard [6] sequence[3] generates a time-spread OCDMA waveform that is modulated with information using on-off keying (OOK). The M downlink signals and the unmodulated "even comb" are combined onto a single fiber and conveyed through the network to each user's optical network unit (ONU). A second fiber conveys the unencoded odd comb to each ONU to serve as local oscillator. Key to the performance of this configuration is the use of *phase and polarization diversity combining* (PPD) in conjunction with the SPC-encoded local oscillator to demodulate coherently the selected received signal. As details below will show, common mode noise and interference are eliminated by the balanced detectors in the PPD circuit, thus reducing MAI essentially to zero.

In the same manner, each ONU encodes the even comb from the first fiber with its unique sequence, OOK modulates this encoded comb with its data, and sends this uplink signal to the OLT via the second fiber.

[1]Demultiplexing is achieved by using a Mach-Zehnder interferometer with a free spectral range equal to twice the repetition rate of the mode locked laser. Therefore the repetition rate of the laser should be one half of the signal repetition rate. Alternatively one can also do the splitting using an edge filter.

[2]The encoder is essentially the one used by Weiner [?].

[3]Any orthogonal sequence set can be used.

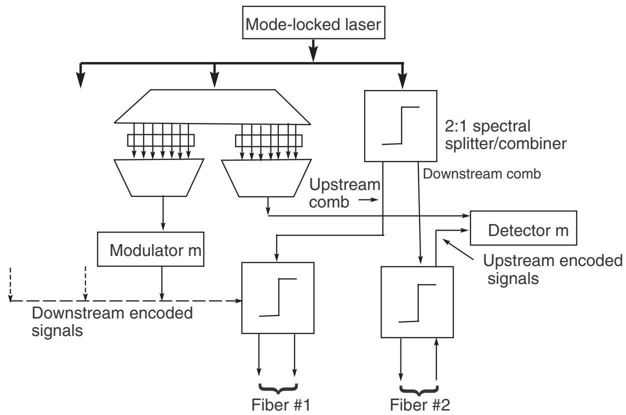

Fig. 1. Optical line termination unit (OLT)

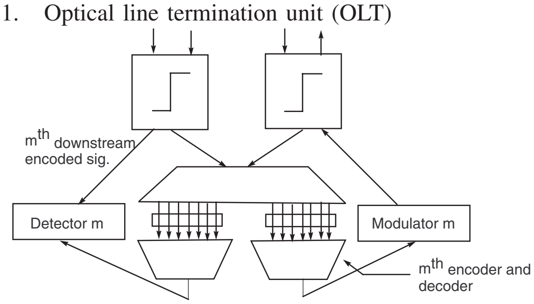

Fig. 2. User's optical network unit (ONU)

The salient features of the proposed architecture are (1) the use of a *single laser* as the source of all transmitted and reference signals and (2) the requirement for only two fibers to achieve all network communications, including the distribution of all reference signals necessary for "full duplex" network operation. Thus, it affords an attractive structure for passive optical networks (PON). The optical receiver uses PPD combining to achieve coherent correlation of the spectrally encoded LO with the received signal ensemble, thus avoiding costly and complex nonlinear threshold detection.

III. OCDMA Performance and MAI

To generate the m^{th} user's signal $s_m(t)$, an AWG demultiplexer [7] spatially decomposes the flattened optical comb; thermal phase shifters [8] phase encode each symbol $C_m^{(n)}$ of a Hadamard sequence onto a distinct spectral line; and a second AWG recombines the encoded spectrum to produce the encoded comb $c_m(t) = \sum_{n=-N/2}^{N/2-1} C_m^{(n)} e^{j\omega_n t},\ m = 1, 2, \ldots, M,\ \omega_n = \omega_0 + 2\pi n/T,\ C_m^{(n)} = \pm 1$ for BPSK, N is the sequence length, and T is the bit interval. Modulating with the data bit A_m gives $s_m(t) = A_m c_m(t)$.

The receiver LO is encoded with the target user's sequence. The LO and the input beams each split into orthogonal polarizations and the phase of each LO polarization beam is shifted by $\pi/2$. These 8 pairs of polarization components are pairwise mixed (Fig. 3) in the PPD combiner to remove phase and polarization fluctuations between the LO and the received signal.

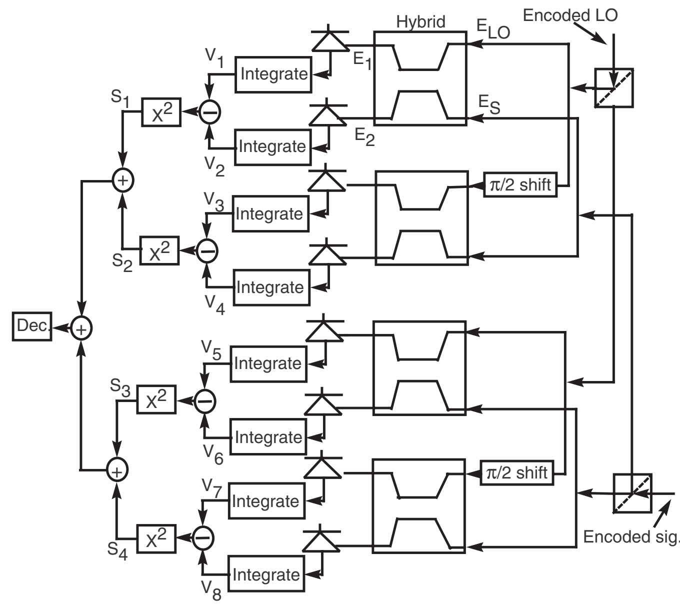

Fig. 3. Phase and Polarization Diversity Combiner

The key to producing very low MAI is the use of the PPD combiner (Fig. 3) to remove speckle and neutralize the phase uncertainty. To see how this occurs, use the top detector as an example. The two inputs to the top optical hybrid are the LO and the composite signal (sum of the signals from M users); their electric fields are given by (1a) and (1b), respectively, where M is the number of

$$E_S(t) = \sqrt{P_S}\cos\theta_S \sum_{m=1}^{M} A_m e^{j(\omega t + \phi_m)} c_m(t) \quad \text{(1a)}$$

$$E_\ell(t) = \sqrt{P_{LO}}\cos\theta_\ell e^{j(\omega t + \phi_\ell)} c_\ell(t) \quad \text{(1b)}$$

users, subscripts S and ℓ denote channel and local oscillator signals, respectively; P, ω, and ϕ are optical power, carrier angular frequency, and phase, respectively; A_m is the data bit (0 or 1) for the m^{th} signal and θ is the angle between the polarization plane and the x axis; c_m is the m^{th} user's signature sequence, and $(1/T)\cdot\int_0^T c_m c_n^* dt = \delta_{mn}$ for orthogonal sequences. The electrical fields at the hybrid outputs are E_1 and E_2:

$$\begin{aligned} E_1 &= \frac{E_\ell}{2} + j\frac{E_S}{2} \\ E_2 &= \frac{E_S}{2} + j\frac{E_\ell}{2} \\ &= j\left(\frac{E_\ell}{2} - \frac{E_S}{2}\right) \end{aligned}$$

The optical powers into the top two detectors are developed in (2), and for OOK, the terms of (2) are as

$$\begin{aligned} P_1 &= |E_1|^2 = \left|\frac{E_\ell}{2} + j\frac{E_S}{2}\right|^2 \\ &= \frac{1}{4}\left(|E_S|^2 + |E_\ell|^2 + jE_S E_\ell^* - jE_S^* E_\ell\right) \\ P_2 &= |E_2|^2 = \left|\frac{E_S}{2} + j\frac{E_\ell}{2}\right|^2 \\ &= \frac{1}{4}\left(|E_S|^2 + |E_\ell|^2 + jE_S^* E_\ell - jE_S E_\ell^*\right) \end{aligned} \quad (2)$$

shown in (3) where the phase difference is written as as

$$\begin{aligned} |E_S|^2 &= P_S \cos^2\theta_S \sum_{m=1}^{M} A_m \quad \text{(signal power)} \\ &+ P_S \cos^2\theta_S \sum_{m-1}^{M} \sum_{\substack{n=1 \\ n\neq m}}^{M} A_m A_n e^{j(\phi_m-\phi_n)} c_m c_n^* \\ &+ c.c. \quad \text{(beating among signals)} \\ |E_\ell|^2 &= P_{LO}\cos^2\theta_\ell \quad \text{(LO power)} \\ jE_S E_\ell^* &= j\sqrt{P_S P_{LO}}\cos\theta_S\cos\theta_\ell \\ &\cdot \sum_{m=1}^{M} A_m e^{j\phi_{m-\ell}} c_m(t) c_\ell^*(t) \\ -jE_S^* E_\ell &= -j\sqrt{P_S P_{LO}}\cos\theta_S\cos\theta_\ell \\ &\cdot \sum_{m=1}^{M} A_m e^{-j\phi_{m-\ell}} c_m^*(t) c_\ell(t) \end{aligned} \quad (3)$$

$\phi_{m-\ell} \triangleq \phi_m - \phi_\ell$ and observe that, for OOK, $A_m^2 = A_m$. Summing the four terms (and writing c_m for $c_m(t)$) gives $4P_1$ which is simplified by letting $\theta_\ell = \pi/4$[4].

$$\begin{aligned} 4P_1(t) &= [j\sqrt{P_s P_{LO}}\cos\theta_S\cos\theta_\ell \\ &\cdot \sum_{m=1}^{M} A_m e^{j\phi_{m-\ell}} c_m c_\ell^* + c.c.] \\ &+ P_{LO}\cos^2\theta_\ell + P_S\cos^2\theta_S \sum_{m=1}^{M} A_m \\ &+ [P_S\cos^2\theta_S \sum_{m=1}^{M} \sum_{\substack{n=1 \\ n\neq m}}^{M} A_m A_n e^{j\phi_{m-n}} c_m c_n^* \\ &+ c.c.] \end{aligned} \quad (4)$$

[4]Until this point, the value of θ_ℓ is arbitrary. Although it is fixed from here onward, the only effect is to make more complicated the coefficients in (9) and (10).

$$\begin{aligned} P_1(t) &= \frac{1}{4}[j\sqrt{P_S P_{LO}}\cos\theta_S\left(\frac{\sqrt{2}}{2}\right) \\ &\cdot \sum_{m=1}^{M} A_m e^{j\phi_{m-\ell}} c_m c_\ell^* + c.c.] \\ &+ \frac{P_{LO}}{8} + \frac{P_S}{4}\cos^2\theta_S \sum_{m=1}^{M} A_m \\ &+ [\frac{P_S}{4}\cos^2\theta_S \sum_{m=1}^{M} \sum_{\substack{k=1 \\ k\neq m}}^{M} A_m A_k e^{j\phi_{m-k}} c_m c_k^* \\ &+ c.c.] \end{aligned} \quad (5)$$

Symmetrically similar expressions for P_2 through P_8 can be derived. Integrating the outputs of the detector over the bit interval T gives

$$V_h = \int_0^T R P_h(t) dt, \;\; h = 1, 2, \cdots, 8$$

where R is the responsivity (current per unit input power) of the photodiode. The integral of the last term in (5) is zero under perfect orthogonality; the second and third terms are constant; and the integral of the first term is:

$$\frac{jR\sqrt{P_S P_L}}{4}\cos\theta_S \frac{\sqrt{2}}{2} e^{j\phi_{n-\ell}} A_n T + c.c.] \quad (6)$$

Therefore,

$$\begin{aligned} V_1 &= \frac{jR\sqrt{P_S P_{LO}} A_n T}{4\sqrt{2}} \cos\theta_S 2\sin\phi_{n-\ell} \\ &+ \frac{R P_{LO} T}{8} + \frac{R P_S T}{4}\cos^2\theta_S \sum_{m=1}^{M} A_m \end{aligned} \quad (7)$$

and similarly for $V_2 - V_8$. Then each of the four partial sums (see Fig. 3) has the form

$$V_1 - V_2 = -R\sqrt{P_S P_{LO}/2} T A_n \cos\theta_s \sin\phi_{n-\ell} \quad (8)$$

and squaring gives

$$S_1 = \frac{1}{2} R^2 P_S P_{LO} T^2 A_n \cos^2\theta_S \sin^2\phi_{n-\ell}. \quad (9)$$

Finally, the estimate of the received bit is obtained by the summation

$$\begin{aligned} \hat{Y}_n &= \sum_{i=1}^{4} S_i \\ &= \frac{1}{2} R^2 P_S P_{LO} T^2 A_n. \end{aligned} \quad (10)$$

The signature of user m is $c_m(t) = e^{j\omega_0 t + \phi_m} \sum_{i=1}^{N} C_m^{(i)} e^{j\omega_i t}$ where ω_0 is the carrier wave angular frequency, ϕ_m is the phase of the m^{th} user signal, N is the length of the CDMA sequence, $C_m^{(i)}$ is the value of the i^{th} chip of the m^{th} user signal, $\omega_i = 2\pi i/T$ is the angular frequency selected by leg i of the AWG, and T is the bit duration. The signatures

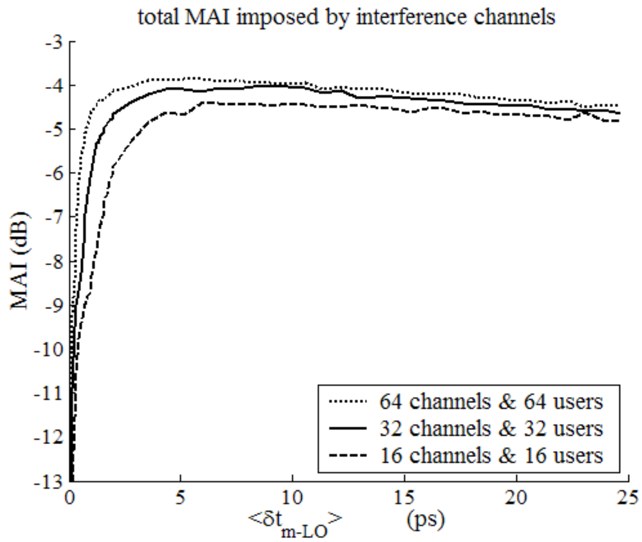

Fig. 4. MAI for fully loaded system

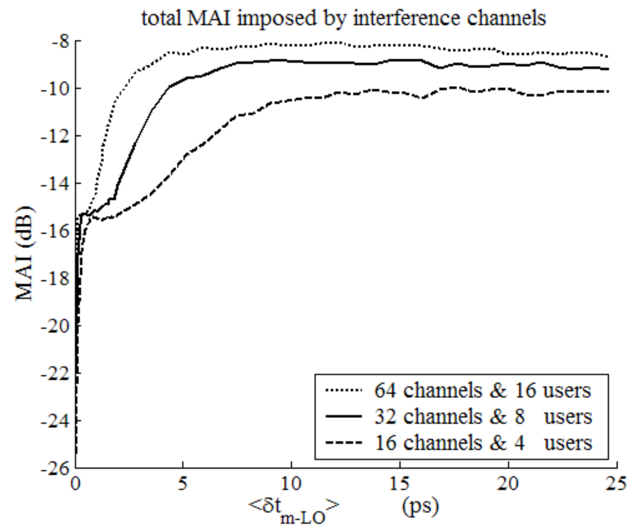

Fig. 5. MAI for partially loaded system, $M = N/4$

c_m are orthogonal if the user signals are completely synchronized at the receiver; *i.e.*, the *cross correlation function* in (11) is 0 *iff* $m \neq n$.

$$\begin{aligned} & \frac{1}{T}\int_0^T c_m(t)c_n^*(t)dt \\ = \; & e^{j(\phi_m-\phi_n)}\sum_{i=1}^{N} C_m^{(i)}C_n^{(i)*} \end{aligned} \tag{11}$$

For a symbol and chip synchronous system (zero delay), there is no MAI, since the coded signals remain orthogonal. However, various impairments, variations in component parameters, and applications that do not admit precise synchronization can result in asynchronous reception that destroys signal orthogonality. Now write the propagation delay between the LO and the m^{th} user signal as the sum of two parts:

$$\Delta t_{m-\ell} = \delta t_{m-\ell} + (\phi_m - \phi_\ell)\omega_0^{-1} \tag{12}$$

The phase term $(\phi_m - \phi_\ell)\omega_0^{-1}$ is fixed by the phase and polarization diversity design. The larger part $\delta t_{m-\ell} = 2\pi\mathcal{I}\omega_0^{-1}$ corresponds to an integer number $\mathcal{I}$ of carrier periods and will result in MAI, whenever the sequences are orthogonal only when perfectly aligned in time. Otherwise, the correlation integral over $[(k-1)T, kT]$ integrates the product of a full LO sequence with the last portion of the sequence for bit $k-1$ and the first portion of the sequence encoding the k^{th} bit. Now the correlation integral of (11) becomes:

$$\begin{aligned} & \frac{1}{T}\int_0^T c_m(t-\delta t_{m-\ell})c_\ell^*(t)dt \\ = \; & \frac{A_m^{(k-1)}}{T} e^{j(\phi_m-\phi_\ell)}\sum_{i=1}^{N}\sum_{s=1}^{N} C_m^{(i)}C_\ell^{(s)*}e^{-j\omega_i\delta t_{m-\ell}} \\ & \cdot \int_0^{\delta t_{m-\ell}} e^{-j(\omega_i-\omega_s)t}dt \\ & + \frac{A_m^{(k)}}{T} e^{j(\phi_m-\phi_\ell)}\sum_{i=1}^{N}\sum_{s=1}^{N} C_m^{(i)}C_\ell^{(s)*}e^{-j\omega_i\delta t_{m-\ell}} \\ & \cdot \int_{\delta t_{m-\ell}}^{T} e^{-j(\omega_i-\omega_s)t}dt \end{aligned} \tag{13}$$

But the system is *chip and frame synchronous*, so the summations are over a common index and (13) simplifies to

$$\begin{aligned} & \frac{1}{T}\int_0^T c_m(t-\delta t_{m-\ell})c_\ell^*(t)dt \\ = \; & \left[A_m^{(k-1)}\delta t_{m-\ell} + A_m^{(k)}(T-\delta_{m-\ell}\right] \\ & \cdot \frac{e^{j(\phi_m-\phi_\ell)}}{T}\sum_{i=1}^{N} C_m^{(i)}C_\ell^{(k)*}e^{-j\omega_i\delta t_{m-\ell}} \end{aligned} \tag{14}$$

When $c_\ell(t) \neq c_m(t)$, (14) represents the MAI caused by the m^{th} user. The MAI was numerically modeled as a function of the mean synchronization delay between the LO and the interfering signals. The signal channel is always assumed to be synchronous with the LO via clock recovery. Two cases were considered: a fully loaded system $(M = N)$ with M asynchronous 10 Gb/s users and N OCDMA channels, and a more lightly loaded system $(M = N/4)$. The relative phases of the LO and interferers are all random, as are the data bit values.

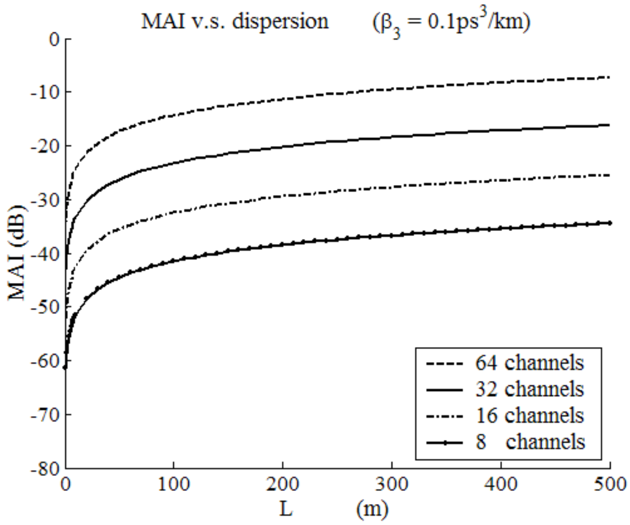

Fig. 6. MAI vs fiber dispersion, zero dispersion fiber

Clearly, the MAI quickly rises from the very low level to a steady value of roughly -4dB for $M = N$ (Fig. 4) and between -8dB and -12dB for $M = N/4$ (Fig. 5). This is easy to understand: when mean synchronization delay $\delta t_{m-\ell}$ exceeds T/N $1.6ps$, the MAI is merely a sum of $MN/2$ random variables (On average, one half of the interferers are transmitting a "1."). Hence, the mean MAI should be $\sim \sqrt{MN/2} \sim N\sqrt{M/2N}$, and the signal to MAI ratio is approximately $\sqrt{M/2N}$. In fact, this is clearly the level at which this ratio saturates in Figs 4 and 5.

As seen, the impairment-free, fully synchronous system produces no MAI, and the channel capacity [9] is determined solely by the channel noise [10] and impairments. For $M \leq N$, capacity is achieved by orthogonal sequences and, for $M > N$, by sequence "multisets" that meet Welch's [11] lower bound [10].

MAI increases in the asynchronous case because partially non-aligned sequences, *e.g.,* $c_m(t + \delta t_{m-\ell})$ and $c_\ell(t)$ are generally not orthogonal. Eq, (11) shows that the correlation computed by the PPD is proportional to the sum $\sum_{i=1}^{N} C_m^{(i)} C_n^{(i)*}$ where $C_m^{(i)}$ is the i^{th} spectral coefficient of the m^{th} signature sequence. Because the spectrum is flattened, these correlation terms are determined solely by the sequence and, since arbitrary cyclic shifts of Hadamard sequences are not orthogonal; *i.e.,* $\sum_{i=1}^{N} C_m^{(i)} C_n^{(j)*} \neq 0,\ i \neq j$, capacity limiting MAI results. Fortunately, if the pairwise correlations of a signature set meet a demonstrated lower bound on *total squared asynchronous correlation (TSAC)*, then the channel capacity of the asynchronous CDMA system is the same as that of the synchronous system [12]. Thus, *for a properly chosen sequence set, the capacity limiting MAI is caused solely by component impairments.*

IV. Impairments

The orthogonality condition $(1/T) \cdot \int_0^T c_m c_n^* dt = \delta_{mn}$ between the different sequences is violated because of various impairments.

A. Dispersion

Reach and capacity of fiber optic systems are limited by dispersion and nonlinearity [1]. When serving 64 users at 10 Gb/s, the proposed system will occupy over 640 GHz of spectrum, the equivalent of a time-based system with $\sim 1.6ps$ pulses. Therefore, chromatic dispersion is expected to be a defining limiting factor. With no dispersion compensation and $\beta_2 = 20ps^2$/km, the reach will be about 0.128 km or 128 meters, but with dispersion compensation, say $\beta_3 = 0.1ps^3$/km, the reach grows to about 40 km. Actually, dispersion is crucial in both spectrally based and time based systems. For SPC, additional phase delay for each frequency is reflected in the correlation expression (15) where the loss of orthogonality is evident. In the time based system,

$$\sum_{i-1}^{N} C_m^i C_n^{j*} e^{j\beta_2(\omega_i - \omega_0)^2 (L_m - L_\ell)/2} \qquad (15)$$

the peak power in the pulse detected by the nonlinear threshold device goes down and threshold detection fails.

Improvement in reach offered by zero-dispersion fiber is explained by computations of MAI due to fiber dispersion in fully synchronized systems (Fig 6). For zero dispersion fiber, this MAI is 10 to 30 dB less for zero-dispersion fiber at 100m, and the growth seems slower with distance.

B. Nonlinearity

The impact of nonlinearity is best understood in the temporal domain. As the signal propagates along the fiber, self phase modulation takes place and the time-dependent phase shift causes the total signal envelope to have a high peak to average power ratio that, in principle, causes increased MAI. However, for the typical PON length of a few km and total power of a few mW, MAI caused by nonlinearity is small factor, as evidenced in Fig. 7 for receipt of a binary "1." Unlike the signal, the frequency comb does experience large nonlinearity because it has high peak powers approaching hundreds of mW, but the impact is limited mostly limited to spectral broadening of the pulse with insignificant consequences.

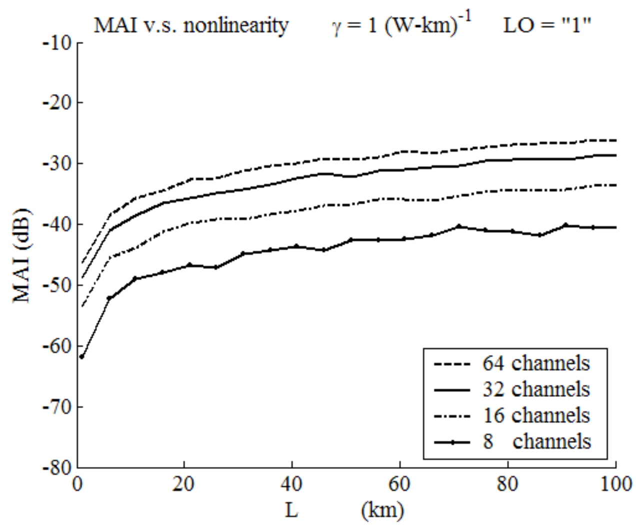

Fig. 7. MAI vs Nonlinearity, LO = ”1”

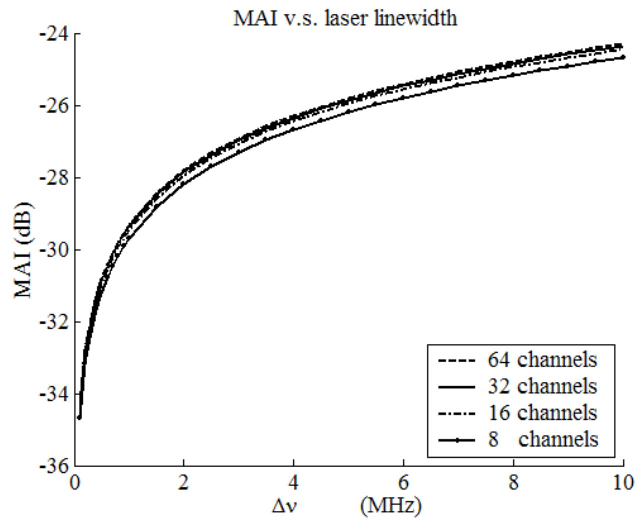

Fig. 8. MAI vs laser linewidth

C. Laser Line Width

The impact of finite laser line width $\Delta\nu_{laser}$ on the coherent system is also best estimated in time domain. In general, the signal and LO are not synchronized to within one bit (*i.e.*, 2 cm of path difference) since they propagate in different fibers. Therefore, in addition to the fixed phase shift between the signal and LO (which is taken care of by phase diversity), there exists a random phase shift $\Delta\phi_{m-\ell}(\tau, \Delta\nu_{laser}$ whose mean value is $\sqrt{\Delta\nu_{laser} t}$ where $0 < \tau < T$. For a 100 ps bit duration it appears that the laser with linewidth less than say 10MHz should suffice, as is shown in Fig 8.

V. Conclusions

PPD in the bit-synchronous case cancels the MAI nearly completely in the absence of impairments. Thus, there are virtually no interfering, random-phase signals in the photodetector to generate speckle noise. The data show that, for very small differences in received bit times, the MAI is quite low, implying large values for spectral efficiency. But the asynchronous cross-correlations exact a significant penalty, as the data show. In certain applications, error control codes can be used to recover a low *b.e.r*. Further, the existence of asynchronously near-orthogonal sequences may afford an additional solution for the asynchronous case but, they must be used with care.

The design achieves good spectral efficiency, a high degree of security, and soft degradation without using a nonlinear optical threshold device or a PLL and leads to flexible and potentially secure networks [13]. Nonlinearity and laser line width have been shown not to be serious impairments when compared with to dispersion.

References

[1] G. Agrawal, *Fiber-Optic Communications Systems*. New York: Wiley Inter-Science, 2002.

[2] R. Scott *et al.*, “Demonstration of an error-free 4 10 Gb/s multiuser spects o-cdma network testbed,” *ptl*, vol. 16, pp. 2186–88, sep 2004.

[3] C. Lam *et al.*, “Experimental demonstration of bipolar optical CDMA system using a balanced transmitter and complementary spectral encoding,” *ptl*, vol. 10, pp. 1504–1506, oct 1998.

[4] A. Pham, N. Miki, and H. Yashima, “Spectral-amplitude-encoding optical-code-division-multiplexing system with a heterodyne detection receiver for broadband optical multiple-access networks,” *J. Optical Networking*, vol. 4, pp. 621–31, oct 2005.

[5] M. Rochette *et al.*, “Gain equalization of EDFAs with Bragg gratings,” *ptl*, vol. 11, pp. 536–8, 1999.

[6] C. Liu, *Introduction to Combinatorial Mathematics*. new york: McGraw-Hill, 1968.

[7] T. Mizuno *et al.*, “Low-loss 1.5 %-Δ arrayed waveguide grating with narrow laterally tapered spotsize converter,” *elet*, vol. 37, pp. 1452–4, 2002.

[8] Y.Inoue, K. Katoh, and M. Kawachi, “Polarization sensitivity of a silica waveguide thermooptic phase shifter for planar lightwave circuits,” *ptl*, vol. 4, pp. 36–8, jan 1992.

[9] C. Shannon, “A mathematical theory of communication,” *bstj*, vol. 27, pp. 379–423, jul 1948.

[10] M. Rupf and J. Masseyj, “Optimum sequence multisets for synchronous code-division multiple-access channels,” *it*, vol. 40, jul 1994.

[11] L. Welch, “Lower bounds on the maximum crosscorrelation of signals,” *it*, vol. 20, may 1974.

[12] S. Ulukus and R. Yates, “User capacity of asynchronous CDMA systems with matched filter receivers and optimum signature sequences,” *it*, vol. 50, pp. 903–09, may 2004.

[13] A. B. Cooper III and J. B. Khurgin, “Phase and polarization diversity for OCDMA,” in *Conference on Lasers and Electro Optics (CLEO) ’06*, Optical Soc. of Amer., 2006.